

# The single-mode description of the integer quantum Hall state with dipole-dipole interaction

Rui-Zhi Qiu<sup>1,2</sup>, Zi-Xiang Hu<sup>3</sup>, and Xin Wan<sup>1</sup>

<sup>1</sup>*Zhejiang Institute of Modern Physics, Zhejiang University, Hangzhou 310027, P.R. China*

<sup>2</sup>*Science and Technology on Surface Physics and Chemistry Laboratory,  
P.O. Box 718-35, Mianyang 621907, Sichuan, P.R. China and*

<sup>3</sup>*Department of Physics, Chongqing University, Chongqing 400044, P.R. China*

(Dated: June 6, 2018)

A topological phase can often be represented by a corresponding wavefunction (exact eigenstate of a model Hamiltonian) that has a higher underlying symmetry than necessary. When the symmetry is explicitly broken in the Hamiltonian, the model wavefunction fails to account for the change due to the lack of a variational parameter. Here we exemplify the case by an integer quantum Hall system with anisotropic interaction. We show that the single-mode approximation can introduce a variational parameter for a better description of the ground state, which is consistent with the recently proposed geometric description of the quantum Hall phases.

## I. INTRODUCTION

The integer quantum Hall (IQH) effect is now regarded as a simple class of topological insulators with broken time-reversal symmetry. A system in such a phase has invariant properties of its ground state wavefunction under smooth deformations of the Hamiltonian. This, of course, does not mean that the ground state wavefunction itself is invariant. For convenience, we often choose to study the system with continuous symmetries in translation and/or rotation in which the ground state wavefunction is relatively simple, although these symmetries are unnecessary for the study of the topological properties. In fact, such a choice can sometimes hide important physics.

Consider an IQH system in the disk geometry with rotational symmetry. Electrons in a polarized lowest Landau level (LLL) fill up ring-shaped orbitals  $\phi_m(z) = z^m e^{-|z|^2/4}$ , where  $z = x + iy$  is the complex coordinate on the plane. The trivial many-body ground state is the Slater determinant of the orbitals with the lowest possible  $m$

$$\Phi_0(z_1, \dots, z_N) = \left[ \prod_{i < j} (z_i - z_j) \right] e^{-\sum_i |z_i|^2/4}, \quad (1)$$

which is the well known Vandermonde determinant multiplied by the ubiquitous Gaussian factor. The wavefunction, which vanishes when two electrons coincide with each other, manifests the Pauli exclusion principle. The trivial many-body state is known to be the ground state even in the presence of interaction.

This prompts some interesting questions. Can effects of interaction be explicitly manifested in the robust IQH state? If yes, how do they modify the ground state wavefunction variationally? These questions can be likewise asked for the fractional quantum Hall (FQH) states, which have been explored in recent experiments using tilted magnetic fields.<sup>1,2</sup> In fact, such attempts have been made recently in the context of the geometric description of FQH states,<sup>3,4</sup> which can be applied straightforwardly to the IQH counterpart.

To construct a variational wavefunction for correlated systems from its noninteracting counterpart is a long-standing problem.<sup>5</sup> Suppose we decompose a many-body Hamiltonian

to be  $H = H_0 + H_1$ . We assume that we know the ground state  $|\Phi_0\rangle$  of  $H_0$ , which describes, for the present discussion, the noninteracting part of the total Hamiltonian.  $H_1$  describes the interparticle interaction. How can the ground state wavefunction be variationally constructed? Within the single-mode approximation, which replaces the effect of  $H_1$  by a single, mean excitation energy  $\omega_0$ , we can write down an ansatz wavefunction  $|\Psi_0\rangle = e^{-H_1/\omega_0}|\Phi_0\rangle$  for the ground state of  $H$ .<sup>5</sup> Here,  $\omega_0$  can be tuned as a variational parameter to minimize the ground state energy. A well-known example is the Gutzwiller's wavefunction,<sup>6</sup> which accounts for the electron correlation in the on-site Hubbard model. An improved independent-mode approximation can lead to Jastrow's ansatz for a trial ground-state wavefunction

$$\Psi_0(\mathbf{r}_1, \dots, \mathbf{r}_N) = e^{\sum_{ij} f(\mathbf{r}_i - \mathbf{r}_j)} \Phi_0(\mathbf{r}_1, \dots, \mathbf{r}_N), \quad (2)$$

where the Jastrow function  $f(\mathbf{r} - \mathbf{r}')$  is determined by energy minimization.<sup>5</sup>

According to the single- and independent-mode approximations, the Jastrow function for the IQH state simply vanishes despite the interparticle interaction. This opinion, of course, is counterintuitive hence oversimplified, especially in the case with anisotropic interaction or mass tensor, as was already discussed by Haldane<sup>3</sup> in the FQH context recently. In this article we take an empirical approach to decipher the IQH ground-state wavefunction from numerical diagonalization of a microscopic system with dipole-dipole interaction. We find that in the IQH regime the realistic ground state can be written as the isotropic IQH ground state multiplied by a sum of a few polynomials, which can be cast in an exponential form much like the Jastrow factor in Eq. (2). The Jastrow factor can be understood as arising, in the single-mode approximation, from an anisotropic quadrupolar interaction. Up to a center-of-mass contribution suppressed by the one-body potential, we show that the wavefunction is consistent with the Bogoliubov transformation of the guiding center coordinates in the isotropic wavefunction. The paper is organized as follows. We introduce our model on quantum Hall systems with dipole-dipole interaction in Sec. II. In Sec. III we analyze the structure of the ground state wavefunction and discuss the regime where it can be understood as a single-mode approximation. We discuss the connection of our findings to recent works on the geometric description on quantum Hall states in

Sec. IV. We summarize the paper in Sec. V and leave some technical details of our calculation in Appendix A.

## II. MODEL

Recent experimental and theoretical development in both dipolar atoms and polar molecules<sup>7</sup> promises us the potential of realizing the FQH effect in systems with tunable and anisotropic interaction.<sup>8–10</sup> In this section we review our model for dipolar atomic systems in the quantum Hall regime and identify the phase of interest in this study.

As proposed in Ref. 11, the fast rotating quasi-two-dimensional gas of polarized fermionic dipoles serves as an ideal arena for the present study. The Larmor theorem states that the fast rotation is equivalent to a high magnetic field for the fermions. Since the p-wave interaction for the polarized fermions is typically small unless in the resonance regime, the only significant interaction in the system is the dipole-dipole interaction. Here without loss of generality, we assumed that the dipole moments are polarized in the  $x$ - $z$  plane of the rotating frame and the motion of all dipoles along  $z$ -axis is frozen to the ground state of the axial harmonic oscillator,  $\phi_z(\zeta) = \pi^{-1/4} q^{-1/2} e^{-\zeta^2/(2q^2)}$ . The quasi-two-dimensional dipole-dipole interaction is described by

$$\begin{aligned} \mathcal{V}_\theta^{(2D)}(x, y) &= c_d V_\theta^{(2D)}(x, y), \text{ where} \\ \mathcal{V}_\theta^{(2D)}(x, y) &= \frac{1}{(2\pi q^2)^{1/2}} \int d\zeta e^{-\zeta^2/(2q^2)} \\ &\times \frac{x^2 + y^2 + \zeta^2 - 3(\zeta \cos \theta + x \sin \theta)^2}{(x^2 + y^2 + \zeta^2)^{5/2}}, \end{aligned}$$

$c_d$  is the interaction strength and  $\theta$  is the polar angle of the dipole moment.

Therefore, within the LLL formalism, we set up a quantum Hall system with anisotropic dipole-dipole interaction as described by the following Hamiltonian

$$H = \alpha L^z + \frac{1}{2} \sum_{m_1, m_2, m_3, m_4} V_{1234}(\theta) f_{m_1}^\dagger f_{m_2}^\dagger f_{m_4} f_{m_3}, \quad (3)$$

where  $f_m^\dagger$  creates a fermion in the state  $\phi_m$  and  $L^z = \sum_m m f_m^\dagger f_m$  is the  $z$ -component of the total angular momentum. The interaction matrix elements  $V_{1234}(\theta)$  are given by

$$\begin{aligned} \int d\mathbf{r} d\mathbf{r}' \psi_{m_1}(\mathbf{r}) \psi_{m_2}(\mathbf{r}') V_\theta^{(2D)}(\mathbf{r} - \mathbf{r}') \psi_{m_3}(\mathbf{r}) \psi_{m_4}(\mathbf{r}') \\ = \cos^2 \theta V_{1234}^z + \sin^2 \theta V_{1234}^x, \end{aligned} \quad (4)$$

where

$$\begin{aligned} V_{1234}^z &= \delta_{m_1+m_2, m_3+m_4} \left[ -4\mathcal{A}_{1234}\mathcal{K}_{1234} \right. \\ &\quad \left. + \frac{1}{3q} \sqrt{\frac{2}{\pi}} \frac{(m_1 + m_2)!}{2^{m_1+m_2} \sqrt{m_1! m_2! m_3! m_4!}} \right], \\ V_{1234}^x &= -\frac{1}{2} V_{1234}^z + \mathcal{A}_{1234}\mathcal{K}_{1234} \delta_{m_1+m_2, m_3+m_4 \pm 2}, \end{aligned}$$

and

$$\begin{aligned} \mathcal{A}_{1234} &= \frac{1}{4\sqrt{2\pi}q} \frac{i^{|m_3-m_1|-|m_4-m_2|}}{2^{(|m_3-m_1|+|m_4-m_2|)/2}} \sqrt{\frac{[m_{13}^<]![m_{24}^<]}{[m_{13}^>]![m_{24}^>]}}, \\ \mathcal{K}_{1234} &= \int dt t^{(|m_3-m_1|+|m_4-m_2|)/2} e^{-t} L_{m_{13}^<}^{|m_3-m_1|} \left( \frac{t}{2} \right) \\ &\times L_{m_{24}^<}^{|m_4-m_2|} \left( \frac{t}{2} \right) \mathcal{E} \left( q\sqrt{\frac{t}{2}} \right). \end{aligned}$$

Here  $m_{ij}^< = \min(m_i, m_j)$ ,  $m_{ij}^> = \max(m_i, m_j)$ ,  $L_m^n(\cdot)$  is the associated Laguerre polynomial, and  $\mathcal{E}(x) = \sqrt{\pi} x e^{x^2} \text{erfc}(x)$  with  $\text{erfc}(\cdot)$  being the complementary error function. From Eq. (4), it is clear that the matrix elements  $V_{1234}(\theta = 0)$  are nonzero for  $m_1 + m_2 - m_3 - m_4 = 0$  and  $V_{1234}(\theta \neq 0)$  are nonzero when  $m_1 + m_2 - m_3 - m_4 = 0$  or  $\pm 2$ .

The details of the potential physical realization of the Hamiltonian were explained in Ref. 11. The isotropic confining potential strength  $\alpha$  can be tuned by the rotation frequency and the tilt angle  $\theta$  by applied electric and magnetic field. We explore, by exact diagonalization, the  $N$ -particle ground state and compute its mean total angular momentum (in units of  $\hbar$ )

$$\overline{M} \equiv \left\langle \Psi^{(N)}(\alpha, \theta) \left| L^z \right| \Psi^{(N)}(\alpha, \theta) \right\rangle \quad (5)$$

where  $\Psi^{(N)}(\alpha, \theta)$  denotes the ground state wave function for given parameters  $\alpha$  and  $\theta$ .

As illustrated in Fig. 1, with isotropic dipole-dipole interaction in the plane of motion, i.e. for  $\theta = 0^\circ$ , the total angular momentum is a good quantum number and can be matched to that of the IQH state  $M_0 = N(N-1)/2$  for  $\alpha > 0.085$  and  $M_L = 3N(N-1)/2$  the  $\nu = 1/3$  Laughlin state for  $\alpha < 0.018$ . Note that we only show  $\alpha > 0.01$  to avoid the unwanted complication due to weak confinement and finite system size. As  $\theta$  increases, the rotational symmetry is explicitly broken and  $\overline{M}$  increases from  $M_0$  to reflect the anisotropy of the interaction. We identify the extended blue region to the up and right of the curved orange dashed line in Fig. 1 to be the anisotropic IQH phase with  $\overline{M} = M_0 + O(1)$ , which has the maximum density in the interior of the oval-shaped droplet.<sup>11</sup>

The introduction of interaction anisotropy breaks the rotational symmetry otherwise present in the disk geometry. This means that we cannot diagonalize the Hamiltonian in the momentum subspace, hence the calculations are restricted to rather small systems. But we have checked out results for  $N = 5-7$  particles and we believe the results presented in the following sections are robust in even larger systems.

## III. DECIPHER THE ANISOTROPIC GROUND-STATE WAVEFUNCTIONS

The isotropic IQH ground state (in a harmonic trap) is the maximum density droplet of electrons in the LLL. One expects that in the presence of small anisotropic interaction the IQH state can only be perturbed at the edge. Hence the

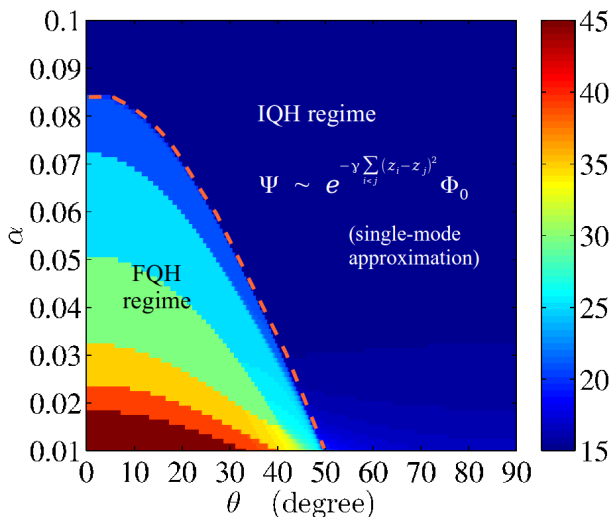


FIG. 1: (Color online) The mean total angular momentum of the ground state  $\overline{M} = \langle \Psi^{(N)}(\alpha, \theta) | L^z | \Psi^{(N)}(\alpha, \theta) \rangle$  (in units of  $\hbar$ ) in a system with  $N = 6$  particles for various confining potential strength  $\alpha$  and tilt angle  $\theta$ . The blue region to the top and right of the orange dashed line represents the anisotropic IQH state, while the rest is loosely referred to as the FQH regime, with the brown region in the lower left corner representing the  $\nu = 1/3$  Laughlin state.

anisotropic IQH state is expected to be the superposition of the isotropic IQH ground state and its edge states. In the following we will first describe the complete basis of edge states in the isotropic case, which will be used later to understand the ground-state wavefunctions in the anisotropic case.

### A. A complete basis in terms of edge states in the isotropic case

Quantum Hall systems have gapless edge states. In the isotropic  $\nu = 1$  integer quantum Hall case the edge states are simply generated by a branch of chiral bosonic modes, which describe the deform of the incompressible quantum Hall droplet at the edge. In the simpler noninteracting case they are generated by electron-hole pair excitations. In terms of analytical wavefunctions they can be written down as the linear combinations of

$$(e_1^{n_1} e_2^{n_2} \dots) \Phi_0 = \left( \prod_{m>0} e_m^{n_m} \right) \Phi_0 \quad (6)$$

with

$$e_0 = 1 \quad (7)$$

$$e_1 = \sum_i z_i \quad (8)$$

$$e_2 = \sum_{i<j} z_i z_j \quad (9)$$

$$e_3 = \sum_{i<j<k} z_i z_j z_k \quad (10)$$

$\vdots$

This is a complete basis for antisymmetric electron wavefunctions, which vanish when  $z_i \rightarrow z_j$ . The convention is when we refer to edge states we focus on those with excitation momentum  $\Delta M = O(1)$ , as oppose to bulk excitations with  $\Delta M = O(N)$ .

To count the edge states, we can define a generation function

$$G(q) = \sum_{\Delta M} q^{\Delta M} \cdot N_{\Delta M} \quad (11)$$

where  $N_{\Delta M}$  is the number of ways to partition  $\Delta M$ , i.e., sets of  $n_m$  such that

$$\Delta M = \sum_{m=0}^{\infty} m n_m \quad (12)$$

It is easy to see that the generation function is

$$G(q) = \prod_{m=1}^{\infty} \frac{1}{1 - q^m}. \quad (13)$$

The number of edge states for  $\Delta M = 0, 1, 2, 3, 4, \dots$  are simply 1, 1, 2, 3, 5, ....

One should notice that the basis we introduced above is not orthogonal. For later numerical analysis it is convenient to introduce the Schur polynomial as an alternative basis. We start with the integer partition,  $N - 1, N - 2, \dots, 0$ , of the ground-state total angular momentum  $M_0 = N(N - 1)/2$ . The ground-state wavefunction  $\Phi_0$  is simply the Slater determinant

$$\begin{aligned} \mathfrak{sl}_{\{N-1, N-2, \dots, 0\}}(\{z_i\}) &= \begin{vmatrix} z_1^{N-1} & z_2^{N-1} & \dots & z_N^{N-1} \\ z_1^{N-2} & z_2^{N-2} & \dots & z_N^{N-2} \\ \vdots & \vdots & \ddots & \vdots \\ z_1^0 & z_2^0 & \dots & z_N^0 \end{vmatrix} \\ &= \prod_{i<j} (z_i - z_j), \end{aligned}$$

multiplied by the ubiquitous Gaussian factor. Naturally, edge excitations are Slater determinants with corresponding partitions of  $M = M_0 + \Delta M$ , and/or their linear combinations. Since different Slater determinants are different occupations of electron orbitals and hence orthogonal to each other, it is

convenient to represent the edge states in terms of Schur polynomials (multiplied by the isotropic ground-state wavefunction). For any integer partition  $\Delta M = d_1 + d_2 + \dots + d_N$ , where  $d_1 \geq d_2 \geq \dots \geq d_N$ , the Schur polynomial is defined as

$$S_{\{d_i\}}(\{z_i\}) = \frac{\mathfrak{sl}_{\{N-1+d_1, N-2+d_2, \dots, 0+d_N\}}(\{z_i\})}{\mathfrak{sl}_{\{N-1, N-2, \dots, 0\}}(\{z_i\})}. \quad (14)$$

For examples,

$$S_1(\{z_i\}) = \sum_i z_i = e_1, \quad (15)$$

$$S_2(\{z_i\}) = \left( \sum_i z_i \right)^2 - \sum_{i < j} z_i z_j = e_1^2 - e_2, \quad (16)$$

$$S_{1,1}(\{z_i\}) = \sum_{i < j} z_i z_j = e_2. \quad (17)$$

where we neglect the trailing zeros in the partition  $\{d_i\}$ . This Schur polynomial basis is found to be most convenient later when we deal with wavefunction overlap and normalization.

### B. Wavefunctions for the edge states in the isotropic case with dipole-dipole interaction ( $\theta = 0$ )

Now we apply the Schur polynomial basis to analyze the isotropic (i.e.  $\theta = 0$ ) IQH ground state and its edge states. For illustration we plot the low-energy spectrum in Fig. 2 for  $N = 6$  particles with isotropic dipole-dipole interaction and  $\alpha = 0.1$ . The state at  $\Delta M = 0$  is the isotropic ground state  $\Phi_0$ , while the rest are the complete edge states up to  $\Delta M = 6$ , as the countings in respective momentum sectors are 1, 1, 2, 3, 5, 7, 11 as expected. Bulk excitations are gapped by the Landau level (LL) spacing, assumed to be infinity in the single LL projection. For  $\Delta M = 1$  there is only one state and obviously

$$\Phi_1^1 = \sum_i z_i \prod_{i < j} (z_i - z_j) e^{-\sum_i |z_i|^2/4} = S_1 \Phi_0. \quad (18)$$

For  $\Delta M = 2$  we have two states, which should be linear combinations of  $S_2 \Phi_0$  and  $S_{1,1} \Phi_0$ . One can see that the combinations

$$\begin{aligned} \Phi_2^1 &= \left[ \sum_i z_i \right]^2 \prod_{i < j} (z_i - z_j) e^{-\sum_i |z_i|^2/4} \\ &= [S_2 + S_{1,1}] \Phi_0, \end{aligned} \quad (19)$$

$$\begin{aligned} \Phi_2^2 &= \left[ \sum_{i < j} (z_i - z_j)^2 \right] \prod_{i < j} (z_i - z_j) e^{-\sum_i |z_i|^2/4} \\ &= [(N-1)S_2 - (N+1)S_{1,1}] \Phi_0 \end{aligned} \quad (20)$$

are the suitable choice, because the latter reduces the interaction energy by allowing higher-degree zeros when any two particles approach each other. One can thus identify the two

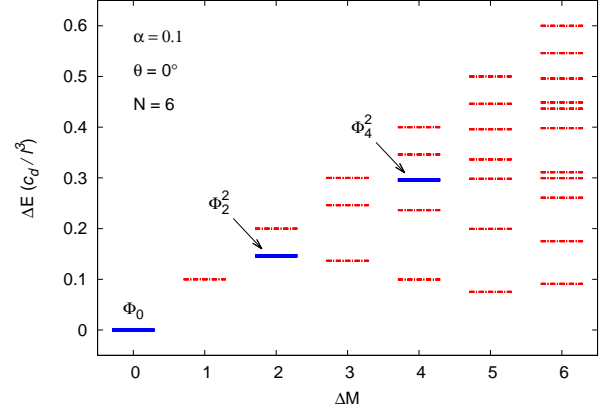


FIG. 2: (Color online) Low-energy excitations for the isotropic IQH state with  $\alpha = 0.1$  and  $\theta = 0^\circ$ . The blue thick levels can be identified as  $\Phi_0$  [Eq. (1)],  $\Phi_2^2$  [Eq. (20)], and  $\Phi_4^2$  [Eq. (21)]. Note that their excitation energies  $\Delta E$  scale with their momenta  $\Delta M$ . These states are the main components of the anisotropic IQH ground state for  $\theta \neq 0^\circ$ .

states in the low-energy spectrum; in particular, the state  $\Phi_2^2$  is labeled in Fig. 2 for later purposes.

One can extend the analysis to higher momentum, which we will not continue here. But we should also highlight, in Fig. 2, another edge state

$$\begin{aligned} \Phi_4^2 &= \left[ \sum_{i < j} (z_i - z_j)^2 \right]^2 \prod_{i < j} (z_i - z_j) e^{-\sum_i |z_i|^2/4} \\ &= [(N-1)^2 S_4 - (N-1)(N+3) S_{3,1} \\ &\quad + 2(N^2+1) S_{2,2} - (N-3)(N+1) S_{2,1,1} \\ &\quad + (N+1)^2 S_{1,1,1,1}] \Phi_0, \end{aligned} \quad (21)$$

whose excitation energy doubles that of  $\Phi_2^2$ , again for later purposes. The other four states in the same momentum sector are other orthogonal linear combinations of  $S_4 \Phi_0$ ,  $S_{3,1} \Phi_0$ ,  $S_{2,2} \Phi_0$ ,  $S_{2,1,1} \Phi_0$ , and  $S_{1,1,1,1} \Phi_0$ . The highest level, e.g., can be identified as  $(\sum_i z_i)^4 \Phi_0$ .

These edge state model wavefunctions are known in earlier literature. For example,  $\Phi_2^2$ , as indicated in the low-lying energy levels for the corresponding isotropic interaction in Fig. 2, is known to be the eigenstate of the projected isotropic interaction in the lowest Landau level.<sup>12</sup> On the other hand,  $\Phi_4^2$  is not necessarily an edge eigenstate for a generic interaction, but the overlap with such a state can be very close to one. For example, in an  $N = 6$  system with isotropic dipole-dipole interaction, the overlap of the corresponding state with  $\Phi_4^2$  is 99.85%. From the form of the wavefunctions, as well as the linear energy-momentum relation, of the states  $\Phi_2^2$  and  $\Phi_4^2$ , the latter can be understood as the corresponding two-boson excitation of the former. We also point out that these edge state wavefunctions are not normalized but their normalization can be straightforwardly worked out (see Appendix A).

### C. Ground-state wavefunctions in the anisotropic case

We now turn to the anisotropic IQH ground state in a harmonic trap, which, for small anisotropy, should be perturbed from the isotropic state at the edge for energetic reasons. Therefore, the anisotropic IQH state is expected to be the superposition of the isotropic IQH ground state and its edge states. Not to be confused with the edge states for the anisotropic ground state, we may call those for the isotropic ground state, which have been discussed in the previous subsection, as *isotropic edge states*. The questions in the following are whether all isotropic edge states contribute, and, if not, how to describe the subset that contributes in a meaningful way.

First of all, due to the nature of the dipole-dipole interaction, only isotropic edge states with an angular momentum difference from the ground state by an integral multiple of 2 can be generated. Therefore, the leading correction must come from either  $\Phi_2^1$  or  $\Phi_2^2$  or both. Numerical analysis reveals that the ground state has vanishingly small overlap with  $\Phi_2^1$ , but substantially large overlap with  $\Phi_2^2$ . This is not surprising, as  $\Phi_2^1$  is a center-of-mass excitation, which is suppressed by the edge confining potential in the disk geometry. On the other hand,  $\Phi_2^2$  distorts the otherwise circular droplet and gains energy from the anisotropic interaction.

We now focus on the regime with  $\overline{M} - M_0 \ll 1$ , in which these edge-state wavefunctions are sufficient for the analysis of anisotropic IQH states. We choose  $\alpha = 0.1$  (the top boundary in Fig. 1) and calculate the overlaps of the ground state  $\Psi^{(N)}(\alpha, \theta)$  with  $N = 6$  obtained from exact diagonalization and  $\tilde{\Phi}_0$ ,  $\tilde{\Phi}_2^2$ , and  $\tilde{\Phi}_4^2$ , the normalized wavefunctions for  $\Phi_0$ ,  $\Phi_2^2$ , and  $\Phi_4^2$ , respectively. In Figure 3(a) we plot  $1 - |\langle \Psi^{(6)}(\alpha, \theta) | \tilde{\Phi}_0 \rangle|^2$  and  $|\langle \Psi^{(6)}(\alpha, \theta) | \tilde{\Phi}_2^2 \rangle|^2$ . For  $\theta$  between 0 and  $90^\circ$  the two curves agree very well and remain small, indicating that the ground state is dominated by  $\Phi_0$ , and the leading correction is  $\Phi_2^2$ . The next correction comes from  $\Phi_4^2$ . Together,  $\Phi_0$ ,  $\Phi_2^2$ , and  $\Phi_4^2$  exhaust almost the whole  $\Psi^{(N)}$  for the strong confinement  $\alpha = 0.1$ , e.g., up to 99.996% at  $\theta = 80^\circ$ . The overlaps of the ground state and other edge states of the isotropic counterpart are essentially zero. For convenience, we also list the values of the significant overlaps at selected angles  $\theta$  in Table I. Therefore, we conclude that, as  $\theta$  increases, the ground state deviates from  $\Phi_0$  to include contributions from  $\Phi_2^2$  and, to a lesser extent,  $\Phi_4^2$  (but essentially not the rest).

Not surprisingly, the overlap with the higher-momentum  $\Phi_4^2$  is much smaller than that with  $\Phi_2^2$ . The question that follows is whether the former can be related to the latter quantitatively. Given the general knowledge of trial wavefunctions for correlated systems, we attempted to fit the numerical wavefunction by

$$\Psi_\gamma = e^{-\gamma \sum_{i < j} (z_i - z_j)^2} \Phi_0 \quad (22)$$

$$= \Phi_0 - \gamma \Phi_2^2 + (\gamma^2/2) \Phi_4^2 + O(\gamma^3) \quad (23)$$

If this is a good trial wavefunction, we expect the  $N$ -particle ground-state wavefunction from exact diagonalization should

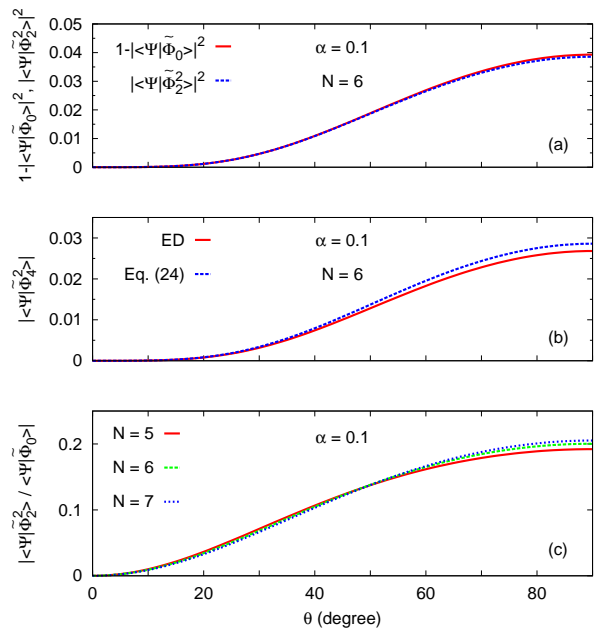


FIG. 3: (Color online) (a) Comparison of  $1 - |\langle \Psi^{(6)}(\alpha, \theta) | \tilde{\Phi}_0 \rangle|^2$  and the leading contribution  $|\langle \Psi^{(6)}(\alpha, \theta) | \tilde{\Phi}_2^2 \rangle|^2$  for a six-particle system. (b) Comparison of  $|\langle \Psi^{(6)}(\alpha, \theta) | \tilde{\Phi}_4^2 \rangle|^2$  obtained from exact diagonalization (ED) and that from the evaluation of Eq. (24), a consequence of the single-mode approximation. (c)  $|\langle \Psi^{(N)}(\alpha, \theta) | \tilde{\Phi}_2^2 \rangle| / |\langle \Psi^{(N)}(\alpha, \theta) | \tilde{\Phi}_0 \rangle|$ , a measure of the anisotropy parameter  $\gamma$ , for  $N = 5-7$ . In all three panels we keep  $\alpha = 0.1$  fixed and vary  $\theta$  only.

$\theta$	$0^\circ$	$20^\circ$	$40^\circ$	$60^\circ$	$80^\circ$
$ \langle \Psi^{(6)}(0.1, \theta)   \tilde{\Phi}_0 \rangle ^2$	1.0000	0.9994	0.9945	0.9865	0.9809
$ \langle \Psi^{(6)}(0.1, \theta)   \tilde{\Phi}_2^2 \rangle ^2$	0.0000	0.0342	0.1042	0.1628	0.1927
$ \langle \Psi^{(6)}(0.1, \theta)   \tilde{\Phi}_4^2 \rangle ^2$	0.0000	0.0008	0.0074	0.0183	0.0258
Computed from Eq. (24)	0.0000	0.0009	0.0079	0.0195	0.0275

TABLE I: Overlaps of the ground state  $\Psi^{(N)}(\alpha = 0.1, \theta)$  obtained by exact diagonalization of an  $N = 6$  system and the normalized wavefunctions  $\tilde{\Phi}_0$ ,  $\tilde{\Phi}_2^2$ , and  $\tilde{\Phi}_4^2$ . For comparison, we also include the overlap with  $\tilde{\Phi}_4^2$  computed from Eq. (24).

follow (see proof in Appendix A)

$$\left| \langle \Psi^{(N)} | \tilde{\Phi}_4^2 \rangle \right| = \sqrt{\frac{N^2 + 1}{2(N^2 - 1)}} \times \frac{\left| \langle \Psi^{(N)} | \tilde{\Phi}_2^2 \rangle \right|^2}{\left| \langle \Psi^{(N)} | \tilde{\Phi}_0 \rangle \right|}. \quad (24)$$

For  $N = 6$  the righthand side can be evaluated to be 0.0009, 0.0079, 0.0195, and 0.0275 for  $\theta = 20^\circ, 40^\circ, 60^\circ$ , and  $80^\circ$ , respectively. The calculated values are in good agreement with the tabulated ones in Table I. In Fig. 3(b) we further compare  $|\langle \Psi^{(6)}(\alpha, \theta) | \tilde{\Phi}_4^2 \rangle|^2$  obtained from exact diagonalization and from Eq. (24) for the whole range of  $\theta$ . The good agreement is thus consistent with the conjecture that the amplitudes of  $\Phi_0$ ,  $\Phi_2^2$ , and  $\Phi_4^2$  in  $\Psi^{(6)}$  are controlled

$\alpha$	0.01	0.03	0.05	0.07	0.09
$ \langle \Psi^{(6)}(\alpha, 70^\circ)   \tilde{\Phi}_0 \rangle ^2$	0.6079	0.8785	0.9440	0.9682	0.9796
$ \langle \Psi^{(6)}(\alpha, 70^\circ)   \tilde{\Phi}_2 \rangle ^2$	0.6139	0.4481	0.3210	0.2464	0.1991
$ \langle \Psi^{(6)}(\alpha, 70^\circ)   \tilde{\Phi}_4 \rangle ^2$	0.4271	0.1568	0.0745	0.0427	0.0276
Compute from Eq.(24)	0.4506	0.1668	0.0794	0.0456	0.0294
Residual weight	0.0712	0.0029	0.0003	0.0001	0.0000

TABLE II: Overlaps of the ground state  $\Psi^{(N)}(\alpha, \theta = 70^\circ)$  obtained by exact diagonalization of an  $N = 6$  system and the normalized wavefunctions  $\tilde{\Phi}_0$ ,  $\tilde{\Phi}_2$ , and  $\tilde{\Phi}_4$ . For comparison, we also include the overlap with  $\tilde{\Phi}_4$  computed from Eq. (24).

by a single parameter  $\gamma$ . In fact, the simplest way to visualize the trend of the parameter  $\gamma$  as a function of  $\theta$  is to plot  $|\langle \Psi^{(N)}(\alpha, \theta) | \tilde{\Phi}_2 \rangle| / |\langle \Psi^{(N)}(\alpha, \theta) | \tilde{\Phi}_0 \rangle|$ , which we show in Fig. 3(c) for different system size  $N = 5-7$ . For practical purposes, it is worth pointing out that as the two-boson excitation  $\tilde{\Phi}_4$  amplitude is already small, the overlaps of the ground-state wavefunction with the three-boson excitation

$$\Phi_6^2 = \left[ \sum_{i < j} (z_i - z_j)^2 \right]^3 \prod_{i < j} (z_i - z_j) e^{-\sum_i |z_i|^2/4}, \quad (25)$$

and beyond are negligible (unless the edge confinement is too weak).

We next turn to the analysis of a sequence of state with increasing  $\alpha$  but fixed  $\theta = 70^\circ$ , in which case we can have  $\bar{M} - M_0 \sim 1$ . Figure 4 repeats the overlap analysis for various  $\alpha$  at the fixed  $\theta$ . In Table II we list the overlap values for selected  $\alpha$  and, for illustration, the residual weight (up to the second order)  $1 - |\langle \Psi^{(N)}(\alpha, \theta) | \tilde{\Phi}_0 \rangle|^2 - |\langle \Psi^{(N)}(\alpha, \theta) | \tilde{\Phi}_2 \rangle|^2 - |\langle \Psi^{(N)}(\alpha, \theta) | \tilde{\Phi}_4 \rangle|^2$ . We find that  $\Psi^{(N)}(\alpha, \theta)$  is still, to a good approximation, composed of  $\tilde{\Phi}_0$ ,  $\tilde{\Phi}_2$ , and  $\tilde{\Phi}_4$ . However, when the edge confinement is weak, higher-order terms may not be negligible and can contribute as much as 7% for  $\alpha = 0.01$  for  $N = 6$ , in which case the weights of  $\tilde{\Phi}_0$  and  $\tilde{\Phi}_2$  are comparable, as indicated in Fig. 4(a). The deviation of  $1 - |\langle \Psi^{(6)}(\alpha, \theta) | \tilde{\Phi}_0 \rangle|^2$  and  $|\langle \Psi^{(6)}(\alpha, \theta) | \tilde{\Phi}_2 \rangle|^2$  indicates that the higher-order terms are vanishingly small, as that we have considered earlier. Nevertheless, Eq. (22) is still a good trial wavefunction, as indicated by the agreement between  $|\langle \Psi^{(N)}(\alpha, \theta) | \tilde{\Phi}_4 \rangle|^2$  calculated from Eq. (24) and directly from the overlap calculation, as shown in Fig. 4(b). Once again, the overlap ratio  $|\langle \Psi^{(N)}(\alpha, \theta) | \tilde{\Phi}_2 \rangle| / |\langle \Psi^{(N)}(\alpha, \theta) | \tilde{\Phi}_0 \rangle|$ , the measure of  $\gamma$ , show very weak size dependence even when the higher-order terms are needed, as plotted in Fig. 4(c).

Thus, in this subsection, we have demonstrated that Eq. (22) is a suitable wavefunction to describe the anisotropic ground state in the IQH regime with dipole-dipole interaction. The decomposition of the anisotropic wavefunction into a sum of the isotropic edge-state wavefunctions allows us to further calculate various properties of the ground state, such as the expectation value of the total angular momentum (which is no longer an integer), as well as the edge Green's function. We will not pursue these straightforward calculations here, but fo-

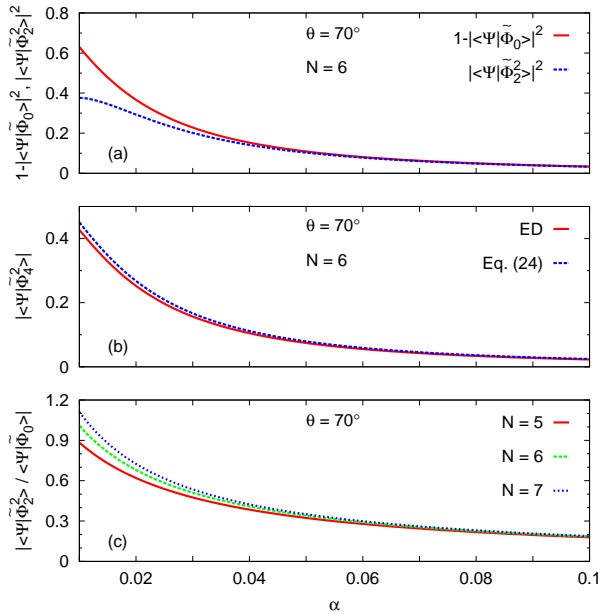


FIG. 4: (Color online) (a) Comparison of  $1 - |\langle \Psi^{(6)}(\alpha, \theta) | \tilde{\Phi}_0 \rangle|^2$  and the leading contribution  $|\langle \Psi^{(6)}(\alpha, \theta) | \tilde{\Phi}_2 \rangle|^2$  for a six-particle system. (b) Comparison of  $|\langle \Psi^{(6)}(\alpha, \theta) | \tilde{\Phi}_4 \rangle|^2$  obtained from exact diagonalization (ED) and that from the evaluation of Eq. (24), a consequence of the single-mode approximation. (c)  $|\langle \Psi^{(N)}(\alpha, \theta) | \tilde{\Phi}_2 \rangle| / |\langle \Psi^{(N)}(\alpha, \theta) | \tilde{\Phi}_0 \rangle|$ , a measure of the anisotropy parameter  $\gamma$ , for  $N = 5-7$ . In all three panels we keep  $\theta = 70^\circ$  fixed and vary  $\alpha$  between 0.01 (weak confinement) and 0.1 (strong confinement).

cus on the understanding of the anisotropy parameter  $\gamma$ .

#### D. The single-mode interpretation for the anisotropic ground-state wavefunction

The form of Eq. (22) exemplifies the independent-mode approximation in Eq. (2) in the IQH context. In particular, since  $\tilde{\Phi}_4$  is the two-boson excitation of  $\tilde{\Phi}_2$ , the wavefunction Eq. (22) can be regarded as a single-mode approximation for the anisotropic IQH state. As discussed in the introduction to the single-mode approximation, we start from the noninteracting Hamiltonian  $H_0 = \alpha L^z$  [the first term of Eq. (3)], which generates the isotropic IQH state Eq. (1) as its ground state. Our wavefunction analysis strongly encourage us to assume, in the spirit of the single-mode approximation, a model quadrupolar interparticle interaction  $V(i, j) = (z_i - z_j)^2$ ; i.e.,  $H_1 = \sum_{i < j} V(i, j)$ . The variational wavefunction Eq. (22) follows naturally as we discussed in the introduction. In the more formal formulation, we can write down a real interparticle interaction

$$V(i, j) = (z_i - z_j)^2 + (\bar{z}_i - \bar{z}_j)^2. \quad (26)$$

The antiholomorphic contribution drops out after the usual LLL projection. Not surprisingly, the real form faithfully

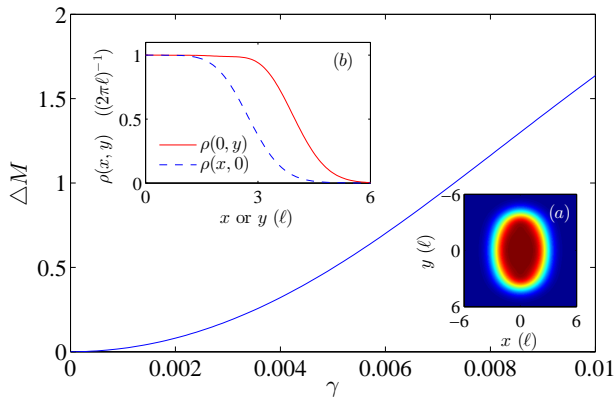


FIG. 5: (Color online) The increase of the mean angular momentum  $\Delta M = \langle \Psi_\gamma | L^z | \Psi_\gamma \rangle - M_0$  with the anisotropy parameter  $\gamma$ . The inset (a) shows the elliptical density profile [in units of  $1/(2\pi\ell^2)$ ] on the  $x$ - $y$  plane when  $\gamma = 0.01$  for an  $N = 6$  system. The inset (b) shows the density profiles along  $x$  and  $y$  axes.

reproduces the angular dependence of the anisotropic component of the dipole-dipole interaction. In the straightforward generalization of the isotropic pseudopotential to the anisotropic case such a quadrupolar interaction is the leading correction. It thus remains to be explored how generic such a model anisotropic wavefunction can be for various interparticle interactions.

The single-mode approach allows us to write down a close form for the variational wavefunction, whose general properties can then be discussed in a quantitative manner. First of all, the rotational invariance of the wavefunction is broken, which means the total angular momentum of the state is no longer a good quantum number. In Fig. 5 we plot the continuous change of the expectation value of the total angular momentum  $\Delta M = \langle \Psi_\gamma | L^z | \Psi_\gamma \rangle - M_0$  as a function of the anisotropy parameter  $\gamma$  for  $N = 6$ . The plot provides a quick way to determine  $\gamma$  from  $\Delta M$  calculated from exact diagonalization. The increase of  $\langle \Psi_\gamma | L^z | \Psi_\gamma \rangle$  with  $\gamma$  comes from the fact that the interaction anisotropy squeezes the otherwise circular droplet into an ellipse, as illustrated by the density profile in the inset (a) of Fig. 5 for  $\gamma = 0.01$ . Away from the edge, the droplet has the maximum density, as in the isotropic case. Note that the sign change of  $\gamma$  would rotate the ellipse by  $90^\circ$ . Alternatively, one can show the density profile along  $x$  and  $y$  axes as in the inset (b) of Fig. 5. Regardless of the elliptical shape, one can still write down the edge states for the anisotropic ground states as edge density fluctuations. In the same single-mode approximation framework, we can write down the edge states as the anisotropic ground state multiplied by symmetrical polynomials. Accordingly, one should observe the low-lying energy-level countings as 1, 1, 2, 3, 5, ... for  $\Delta M \approx 0, 1, 2, 3, 4, \dots$ , respectively. These features have already been reported in the exact diagonalization calculation in Ref. 11 (Fig. 7). It is worth pointing out that the variational wavefunctions in the single-mode approach also allows us to calculate additional properties of much larger systems by variational Monte Carlo simulation.

#### IV. COMPARISON WITH EARLIER WORKS

The consideration of the broken rotational invariance in the quantum Hall context appeared first in the alternative discussion on the effect of anisotropic effective mass tensor<sup>14</sup>. Very recently the joint effects of both anisotropic mass and interaction surfaced in the geometric description of quantum Hall states.<sup>3</sup> Haldane<sup>3</sup> pointed out that the conventional understanding of the Laughlin wavefunctions is not complete; in his novel geometric description the original Laughlin wavefunction is simply a member of a family of Laughlin states, parameterized by a hidden (continuous) geometric degree of freedom. The family of the Laughlin states, with the geometric factor as a variational parameter, potentially provides a better description of the FQH effect in the presence of either anisotropic effective mass or anisotropic interaction, which are present in real materials.

Haldane<sup>3</sup> argued that guiding center metric should be regarded as a variational parameter in the generalized family of Laughlin trial wavefunctions. The family of the variational wavefunction can be constructed by squeezing the LL orbitals.<sup>4</sup> In the symmetric gauge one can introduce a unimodular (or Bogliubov) transformation

$$\begin{pmatrix} z \\ \bar{z} \end{pmatrix} \rightarrow \frac{1}{\sqrt{1-|\lambda|^2}} \begin{pmatrix} 1 & \lambda^* \\ \lambda & 1 \end{pmatrix} \begin{pmatrix} z \\ \bar{z} \end{pmatrix}. \quad (27)$$

of the Landau level (LL) wavefunctions to generate a set of anisotropic single-particle basis states.<sup>11</sup> The unimodular transformation approach also appeared in the consideration of Read and Rezayi<sup>15</sup> on the geometric aspects of the uniform deformation of quantum Hall states in the context of Hall viscosity, which is the nondissipative transport coefficient that describes the stress in the adiabatic response to a strain. The authors<sup>15</sup> pointed out that the extra term in the exponential corresponds to a quadrupolar harmonic perturbation in the plasma mapping for the Laughlin state.<sup>16</sup>

Explicit construction of the family of wavefunctions by the unimodular transformation<sup>4</sup> confirms that the isotropic Laughlin wavefunction is the variational ground state for an isotropic interparticle interaction. In contrast, the dipole-dipole interaction, as occurs in rotating dipolar cold atomic systems, leads to an anisotropic variational ground state.<sup>4</sup> On a torus geometry without boundary, one can calibrate the wavefunction anisotropy or the guiding center metric by exploring static structure factor and pair correlation function.<sup>17,18</sup> The absence of the Jastrow factor for the isotropic IQH state considered in the present work thus can be regarded as a special case of the Laughlin state at filling fraction  $\nu = 1$ . In the geometric description, the metric-deformed single-particle basis can be used to set up the stage for a variational IQH wavefunction<sup>4,15</sup>

$$\Phi_0^\lambda(z_1, \dots, z_N) = e^{-\lambda \sum_i z_i^2/4} \Phi_0(z_1, \dots, z_N), \quad (28)$$

where  $\lambda$  parametrizes the metric change or anisotropy. Note that the extra term in the exponential, which arises from the modification of single-particle basis, will be ubiquitous for

all FQH wavefunctions. Apparently, Eq. (28) differs from Eq. (22) that we found earlier. However, the single-mode (or, more generically, independent-mode) approximation here echoes the geometric description<sup>3</sup> of quantum Hall states in that both quest for a (set of) variational parameter(s) that accounts for the correlation of electrons. It is, therefore, conceivable that for the IQH effect the two descriptions may be unified, at least for the IQH state with dipole-dipole interaction.

Not surprisingly, Eqs. (28) and (22) can be related by noticing

$$\sum_i z_i^2 = \frac{1}{N} \left[ \sum_i z_i \right]^2 + \frac{1}{N} \left[ \sum_{i<j} (z_i - z_j)^2 \right]. \quad (29)$$

One thus concludes that the relative coordinate part of  $\Psi_\gamma$  in Eq. (22) is the same (given  $\gamma = \lambda/N$ ) as that of  $\Phi_0^\lambda$  in Eq. (28), and therefore the two-body interaction energy for the variational state  $\Psi_\gamma$  is the same as that for the variational state  $\Phi_0^\lambda$ . The difference  $e^{-\lambda(\sum_i z_i)^2/N}$  in the anisotropic case, when expanded for small  $\lambda$ , involves  $\Phi_2^1$  and its descendants, which are not generated by the dipole-dipole interaction, as we discussed in the wavefunction analysis. In fact, these terms vanishes for energetic reasons, as the expectation value of the one-body part of the Hamiltonian Eq. (3) for  $\Phi_0^\lambda$  is larger than that for  $\Psi_\gamma$ . For generic edge confinement, the presence of  $\exp[-\lambda(\sum_i z_i)^2/N]$  in  $\Phi_0^\lambda$  leads to larger total angular momentum  $L^z$  and larger energy. In the planer geometry we consider here, one expects that the center-of-mass coordinate and relative coordinates can be decoupled, and the former will then be suppressed by the one-body contributions in the Hamiltonian. Therefore, we conclude that the unimodularly transformed wavefunction for the IQH case is consistent with the single-mode approximation of the anisotropic quadrupolar interaction.

## V. SUMMARY

In summary, we study the evolution of the ground state wavefunction for an IQH droplet with anisotropic dipole-dipole interaction. We perform the numerical anatomy of the ground-state wavefunction and confirmed that a variational wavefunction can be constructed in the single-mode approximation in the anisotropic IQH phase as in the generic treatment for correlated systems. We further argue that the single-mode approximation for the anisotropic interaction is consistent with the geometric description for the anisotropic IQH phase. The present study thus answers, from a different angle, how a certain perturbation (regarded as additional geometric degree of freedom) can be accounted for in the trial wavefunction (otherwise without a variational parameter) for a topological phase. It would be interesting to see such an understanding can apply to other type of interactions and other topological phases.

## Acknowledgments

XW thanks Peter Fulde and Duncan Haldane for the illuminating discussions that motivated this study. The work was supported by the 973 Program under Project Nos. 2009CB929101 and 2012CB927404, the NSFC Project Nos. 11174246 and 11274403, and the Discipline Development Fund Project No. ZDXKFZ201206.

## Appendix A: Proof of Eq. (24)

In this appendix we show that if the numerical obtained ground-state wavefunction  $\Psi^{(N)}(\{z_i\})$  for the anisotropic  $N$ -particle IQH state can be well described by the variational wavefunction

$$\begin{aligned} \Psi_\gamma(\{z_i\}) &= e^{-\gamma \sum_{i<j} (z_i - z_j)^2} \Phi_0 & (A1) \\ &= \Phi_0 - \gamma \Phi_2^2 + (\gamma^2/2) \Phi_4^2 + O(\gamma^3), & (A2) \end{aligned}$$

where  $\gamma$  characterizes the anisotropy, and the unnormalized isotropic components, as illustrated in the main text, are

$$\Phi_0(\{z_i\}) = \left[ \prod_{i<j} (z_i - z_j) \right] e^{-\sum_i |z_i|^2/4}, \quad (A3)$$

$$\begin{aligned} \Phi_2^2(\{z_i\}) &= \left[ \sum_{i<j} (z_i - z_j)^2 \right] \prod_{i<j} (z_i - z_j) e^{-\sum_i |z_i|^2/4} \\ &= [(N-1)S_2 - (N+1)S_{1,1}] \Phi_0, & (A4) \end{aligned}$$

and

$$\begin{aligned} \Phi_4^2(\{z_i\}) &= \left[ \sum_{i<j} (z_i - z_j)^2 \right]^2 \prod_{i<j} (z_i - z_j) e^{-\sum_i |z_i|^2/4} \\ &= [(N-1)^2 S_4 - (N-1)(N+3)S_{3,1} \\ &\quad + 2(N^2+1)S_{2,2} - (N-3)(N+1)S_{2,1,1} \\ &\quad + (N+1)^2 S_{1,1,1,1}] \Phi_0, & (A5) \end{aligned}$$

the overlaps between  $\Psi^{(N)}$  and  $\Phi_0$ ,  $\Phi_2^2$ , and  $\Phi_4^2$  satisfy an equality

$$\left| \langle \Psi^{(N)} | \tilde{\Phi}_4^2 \rangle \right| = \sqrt{\frac{N^2+1}{2(N^2-1)}} \times \frac{\left| \langle \Psi^{(N)} | \tilde{\Phi}_2^2 \rangle \right|^2}{\left| \langle \Psi^{(N)} | \tilde{\Phi}_0 \rangle \right|}, \quad (A6)$$

where  $\tilde{\Phi}_0$ ,  $\tilde{\Phi}_2^2$ , and  $\tilde{\Phi}_4^2$  are normalized wavefunctions of  $\Phi_0$ ,  $\Phi_2^2$ , and  $\Phi_4^2$ , respectively. The proof is basically a bookkeeping of all normalization factors. To begin with, we approximate the normalized numerical ground state by

$$\Psi^{(N)} = \Psi_\lambda / \sqrt{\langle \Psi_\lambda | \Psi_\lambda \rangle} = \mathcal{N}_\lambda \Psi_\lambda. \quad (A7)$$



with

$$\begin{aligned} \frac{1}{\mathcal{N}_\lambda^2} &\equiv \langle \Psi_\lambda | \Psi_\lambda \rangle \\ &= \langle \Phi_0 | \Phi_0 \rangle + \lambda^2 \langle \Phi_2^2 | \Phi_2^2 \rangle + \frac{\lambda^4}{4} \langle \Phi_4^2 | \Phi_4^2 \rangle + O(\lambda^6). \end{aligned} \quad (\text{A8})$$

Given that a Slater determinant  $\mathfrak{sl}_{\{m_i\}}$  in the FQH context is normalized by

$$\frac{1}{\sqrt{N!}} \prod_{i=1}^N \frac{1}{\sqrt{2\pi 2^{m_i} m_i!}}, \quad (\text{A9})$$

we obtain

$$\begin{aligned} &\langle S_{\{d_i\}} \Phi_0 | S_{\{d_i\}} \Phi_0 \rangle \\ &= N! \prod_{i=1}^N (2\pi) 2^{N-i+d_i} (N-i+d_i)! \\ &= 2^{\sum_i d_i} \prod_{i=1}^N \frac{(N-i+d_i)!}{(N-i)!} \langle \Phi_0 | \Phi_0 \rangle. \end{aligned} \quad (\text{A10})$$

Consequently, we find

$$\frac{\langle \Phi_2^2 | \Phi_2^2 \rangle}{\langle \Phi_0 | \Phi_0 \rangle} = 8N^2 (N^2 - 1), \quad (\text{A11})$$

$$\frac{\langle \Phi_4^2 | \Phi_4^2 \rangle}{\langle \Phi_0 | \Phi_0 \rangle} = 128N^4 (N^4 - 1). \quad (\text{A12})$$

With the identification of  $\Psi^{(N)} = \Psi_\gamma = \Phi_0 - \gamma \Phi_2^2 + (\gamma^2/2) \Phi_4^2 + O(\gamma^3)$ , we find

$$\langle \Psi^{(N)} | \Phi_0 \rangle = N_\lambda \langle \Phi_0 | \Phi_0 \rangle, \quad (\text{A13})$$

$$\begin{aligned} \langle \Psi^{(N)} | \Phi_2^2 \rangle &= -\lambda N_\lambda \langle \Phi_2^2 | \Phi_2^2 \rangle \\ &= -8\lambda N_\lambda N^2 (N^2 - 1) \langle \Phi_0 | \Phi_0 \rangle, \end{aligned} \quad (\text{A14})$$

$$\begin{aligned} \langle \Psi^{(N)} | \Phi_4^2 \rangle &= (\lambda^2/2) N_\lambda \langle \Phi_4^2 | \Phi_4^2 \rangle \\ &= 64\lambda^2 N_\lambda N^4 (N^4 - 1) \langle \Phi_0 | \Phi_0 \rangle. \end{aligned} \quad (\text{A15})$$

Finally, we reach the equality

$$\left| \langle \Psi^{(N)} | \tilde{\Phi}_4^2 \rangle \right| = \sqrt{\frac{N^2 + 1}{2(N^2 - 1)}} \times \frac{\left| \langle \Psi^{(N)} | \tilde{\Phi}_2^2 \rangle \right|^2}{\left| \langle \Psi^{(N)} | \tilde{\Phi}_0 \rangle \right|}. \quad (\text{A16})$$

- <sup>1</sup> J. Xia, J. P. Eisenstein, L. N. Pfeiffer, and K. W. West, *Nat. Phys.* **7**, 845 (2011).
- <sup>2</sup> D. Kamburov, Y. Liu, M. Shayegan, L.N. Pfeiffer, K.W. West, and K.W. Baldwin, *Phys. Rev. Lett.* **110**, 206801 (2013).
- <sup>3</sup> F. D. M. Haldane, *Phys. Rev. Lett.* **107**, 116801 (2011).
- <sup>4</sup> R.-Z. Qiu, F. D. M. Haldane, X. Wan, K. Yang, and S. Yi, *Phys. Rev. B* **85**, 115308 (2012).
- <sup>5</sup> P. Fulde, *Electron Correlations in Molecules and Solids*, 3rd ed. (Springer, Berlin, Heidelberg 1995) p. 100.
- <sup>6</sup> M. C. Gutzwiller, *Phys. Rev. Lett.* **10**, 159 (1963).
- <sup>7</sup> For reviews, see M. A. Baranov, M. Dalmonte, G. Pupillo, and P. Zoller, *Chem. Rev.* **112**, 5012 (2012) and the references therein.
- <sup>8</sup> N. R. Cooper, E. H. Rezayi, and S. H. Simon, *Phys. Rev. Lett.* **95**, 200402 (2005).
- <sup>9</sup> M. A. Baranov, K. Osterloh, and M. Lewenstein, *Phys. Rev. Lett.* **94**, 070404 (2005).

- <sup>10</sup> T. Grass, M. A. Baranov, and M. Lewenstein, *Phys. Rev. A* **84**, 043605 (2011).
- <sup>11</sup> R.-Z. Qiu, S.-P. Kou, Z.-X. Hu, X. Wan, and S. Yi, *Phys. Rev. A* **83**, 063633 (2011).
- <sup>12</sup> S. A. Trugman and S. Kivelson, *Phys. Rev. B* **31**, 5280 (1985).
- <sup>13</sup> F. D. M. Haldane, *Phys. Rev. Lett.* **51**, 605 (1983).
- <sup>14</sup> F. D. M. Haldane, in *The Quantum Hall Effect*, eds. R. E. Prange and S. M. Girvin, 2nd ed. (Springer, New York 1990) p. 309.
- <sup>15</sup> N. Read and E. H. Rezayi, *Phys. Rev. B* **84**, 085316 (2011).
- <sup>16</sup> P. Di Francesco, M. Gaudin, C. Itzykson, and F. Lesage, *Int. J. Mod. Phys. A* **9**, 4257 (1994).
- <sup>17</sup> B. Yang, Z. Papić, E. H. Rezayi, R. N. Bhatt, and F. D. M. Haldane, *Phys. Rev. B* **85**, 165318 (2012).
- <sup>18</sup> H. Wang, R. Narayanan, X. Wan, and F.-C. Zhang, *Phys. Rev. B* **86**, 035122 (2012).